Chain-Length-Dependent Termination in *n*-Butyl Methacrylate and *tert*-Butyl Methacrylate Bulk Homopolymerizations Studied via SP-PLP-ESR

Johannes Barth, Michael Buback,* Pascal Hesse, and Tatiana Sergeeva

Institute for Physical Chemistry, University of Göttingen, Tammannstrasse 6, D-37077 Göttingen, Germany

Received September 12, 2008; Revised Manuscript Received November 17, 2008

ABSTRACT: The chain-length dependence of the termination rate coefficient, k_t, of bulk homopolymerizations of *n*-butyl methacrylate (*n*-BMA) and *tert*-butyl methacrylate (*t*-BMA) at ambient pressure and temperatures between −30 and 60 °C has been studied via the single pulse−pulsed laser polymerization−electron spin resonance (SP-PLP-ESR) technique. The decay of radical concentration, c_R, after laser SP initiation is monitored with a high time resolution of microseconds by ESR spectroscopy. Radical chain length, *i*, increases linearly with time *t* after applying the laser pulse. The experimental $k_t^{i,i}$ values refer to rate coefficients for termination of two radicals of identical chain length *i*. The variation of $k_t^{i,i}$ with chain length is adequately represented via the composite model proposed by Smith et al., in which two power-law expressions, $k_t^{i,i} \propto i^{-\alpha}$, are contained with the exponents α_s and α_l referring to short-chain and long-chain radicals, respectively. The transition between the two regimes occurs at the crossover chain length, i_c. The rate coefficients extrapolated for termination of two radicals of chain length unity, $k_t^{1,1}$, are almost identical for *n*-BMA and *t*-BMA with an activation energy of $E_A(k_t^{1,1}) \approx 10$ kJ mol^{-1}. The α_s values are close to each other: 0.65 ± 0.10 (*n*-BMA) and 0.56 ± 0.10 (*t*-BMA). Both α_l values are found to be 0.20 ± 0.05, which is close to the theoretical value of $\alpha_l = 0.16$. The crossover chain lengths are $i_c \approx 50$ for *n*-BMA and $i_c \approx 70$ for *t*-BMA. The minor differences in composite-model parameter values of *n*-BMA and *t*-BMA are assigned to differences in chain mobility.

Introduction

Because of diffusion control, with contributions from translational, segmental, and reaction diffusion, termination is the most complex reaction step in free-radical polymerization.[1] Particularly clear evidence for the termination rate coefficient, k_t, being diffusion controlled is provided by the so-called Norrish−Trommsdorff[2,3] or gel effect, which is caused by a decrease in k_t due to viscosity increasing upon monomer-to-polymer conversion and to a concomitant increase in polymer molecular weight. Mostly chain-length-averaged values for k_t, $\langle k_t \rangle$, have been experimentally determined. The techniques for determination of $\langle k_t \rangle$ as well as the difficulties involved in deducing reliable termination rate coefficients have been recently reviewed.[1,4] Only a few methods for investigations into chain-length-dependent (CLD) termination have been proposed and tested so far. They are based on the control of radical chain length by either using RAFT (reversible addition−fragmentation chain transfer) agents or by applying single pulse−pulsed laser polymerization (SP-PLP) techniques. Under RAFT control, chain length *i* scales with monomer-to-polymer conversion, whereas in SP-PLP, the radical chain length is proportional to the time after applying a laser pulse. With both techniques, narrow chain-length distributions of radicals are established, which enormously simplifies the kinetic treatment, as the multitude of $k_t^{i,j}$ values, referring to termination of two radicals of arbitrary size, essentially reduces to $k_t^{i,i}$, representing the termination of radicals which are identical in chain length. The chain-length dependence of $k_t^{i,i}$ may be represented by the power-law expression

$$k_t^{i,i} = k_t^{1,1} i^{-\alpha} \tag{1}$$

In order to take into account that the chain-length dependence of k_t is more pronounced for shorter chains ($i < i_c$) than for larger radical chain lengths ($i > i_c$), Smith et al.[5] proposed a composite model for $k_t^{i,i}$ at low degrees of monomer conversion, which consists of two such power-law expressions:

$$\begin{aligned} k_t^{i,i} &= k_t^{1,1} \cdot i^{-\alpha_s} && i \le i_c \\ k_t^{i,i} &= k_t^{1,1} \cdot i^{-\alpha_s+\alpha_l} \cdot i^{-\alpha_l} = k_t^0 \cdot i^{-\alpha_l} && i > i_c \end{aligned} \tag{2}$$

The power-law exponents, α_s and α_l, refer to short-chain and long-chain radicals, respectively; i_c is the so-called crossover chain length separating the short-chain and long-chain regimes; k_t^0 is the termination rate coefficient for the hypothetical situation of two radicals of chain length unity terminating by segmental diffusion (see below). CLD termination of short chains is assumed to be governed by center-of-mass diffusion. Thus, α_s may be expected to be in the range 0.5 and 1 with these lower and upper limiting values being associated with center-of-mass diffusion of random coils and of rodlike chains, respectively.[6] Radicals of chain lengths exceeding i_c are less rapidly diffusing and may get entangled which considerably increases the contact time of two such radicals. The associated termination mechanism is denoted as segmental diffusion (SD) control. According to theory, the associated power-law exponent α_l is 0.16.[7−9]

An easy access to model-independent $k_t^{i,i}$ values has been devised and used by Vana et al.[10] Within the so-called RAFT-CLD-T method, the rate of polymerization, R_p, during the course of a RAFT-mediated polymerization is detected via differential scanning calorimetry (DSC). This method is widely applicable, although k_t determination via RAFT-CLD-T is associated with the same difficulties as met in other stationary polymerization techniques: initiator concentration, initiator efficiency, and initiator decomposition rate coefficients need to be known for estimating $k_t k_p^{-2}$, from which the coupled parameter k_t is obtained via the propagation rate coefficient, k_p. The latter coefficient has been determined for most common monomers via the IUPAC-recommended pulsed laser polymerization−size exclusion chromatography (PLP-SEC) method.[11,12] Instationary

* Corresponding author: e-mail mbuback@gwdg.de; Fax 49 551-39-31-44.

10.1021/ma802078g CCC: $40.75
Published on Web 01/05/2009

polymerization experiments, on the other hand, allow for deducing k_t values without the necessity of knowing initiator decomposition rate and initiator efficiency. Thus, the single pulse−pulsed laser polymerization−near-infrared (SP-PLP-NIR) technique[4,13] provides access to termination rate coefficients by analyzing monomer conversion vs time traces which are measured with a time resolution of microseconds after applying a laser single pulse. The fitting procedure directly yields $k_t k_p^{-1}$and thus k_t, as k_p is accessible from PLP-SEC.

The SP-PLP-NIR-RAFT technique which has recently been introduced by our group[14] combines the high accuracy of the SP-PLP-NIR technique with chain-length control by RAFT agents. Hence, accurate model-independent $k_t^{i,i}$ data became available. Both methods, RAFT-CLD-T as well as SP-PLP-NIR-RAFT, have been applied to several monomers such as methyl acrylate,[15−17] butyl acrylate,[14,18] and dodecyl acrylate[17,19] as well as for methyl methacrylate[20,21] and styrene,[10,22] yielding chain-length-dependent k_t data which are in satisfactory agreement.[17,18] There are however some limitations with these two RAFT-based methodologies: For a particular monomer, it may be difficult to find a RAFT agent which ensures radical chain length and monomer conversion being correlated. Moreover, the RAFT agent may affect polymerization kinetics and thus $k_t^{i,i}$, e.g., by giving rise to retardation phenomena.[23] High quality of SP-PLP-NIR-RAFT data, in addition, requires that the monomer is relatively high in k_p and low in k_t. Furthermore, the basic principle of both methods, i.e., the correlation of radical chain length and monomer-to-polymer conversion, induces an inherent ambiguity into the so-obtained termination rate coefficients in that the $k_t^{i,i}$ values may be affected by both chain length and monomer conversion. Thus, within the two RAFT-based methodologies, each degree of polymerization is associated with a different viscosity of the polymerizing system. A decrease in k_t toward higher monomer conversion may be due to both increasing chain length and increasing viscosity. The short-chain regime may be particularly vulnerable toward this problem, as the velocity of center-of-mass diffusion strongly depends on overall viscosity. Hence, both methods may lead to an overestimation of α_s. The difficulties may, at least partly, be overcome by carrying out series of polymerization experiments with widely differing RAFT agent concentrations.

Time-resolved measurement of radical concentration, c_R, after laser single pulse initiation provides the most direct access to CLD termination rate coefficients, as was recently demonstrated by single-pulse laser experiments carried out in conjunction with ESR (electron spin resonance) spectrometric detection of c_R.[24] In principle, this SP-PLP-ESR method allows for model-independent determination of $k_t^{i,i}$ according to eq 3.

$$\frac{dc_R}{dt} = -2k_t^{i,i}{c_R}^2 \qquad (3)$$

Unfortunately, the signal-to-noise quality of SP-PLP-ESR will mostly not be sufficient to provide $k_t^{i,i}$ from differentiation of experimental $c_R(t)$ data. Fitting of kinetic expressions to the measured c_R vs time data, however, allows for adequate estimates of chain-length-dependent k_t.[24−27] An advantage of SP-PLP-ESR is seen in the absence of any additives to the polymerizing system and in the fact that the chain-length dependence may be mapped out at more or less constant conversion. Whereas the parameters of the composite model, i.e., α_s, α_l, and i_c, are directly accessible from SP-PLP-ESR without knowing absolute radical concentration, the estimate of termination rate coefficients requires absolute $c_R(t)$ data to be known. Thus, the ESR setup needs to be calibrated for quantitative measurements of radical concentration. The calibration is based on the proportionality between the double integral of the ESR (dispersion) spectrum, $\int\int I_{SC}$, and radical concentration. The SP-PLP-ESR technique has already been used for determination of $k_t^{i,i}$ in radical polymerizations of dodecyl methacrylate[24,26] (DMA), cyclohexyl methacrylate[26] (CHMA), benzyl methacrylate[26] (BzMA), dibutyl itaconate[25] (DBI), and the butyl acrylate dimer[27] (BAD). These monomers have in common that termination rates are relatively low.

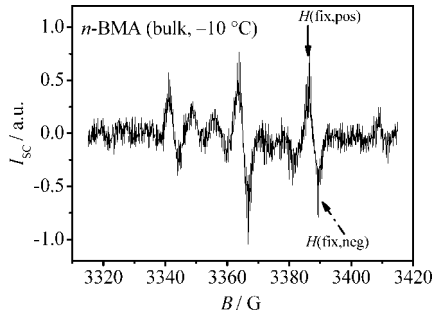

Figure 1. ESR spectrum recorded during pseudostationary pulsed laser-induced polymerization of *n*-butyl methacrylate (*n*-BMA) in bulk at −10 °C. The spectrum was recorded at a sweep time of 10.5 s, a modulation amplitude of 3 G, a microwave power of 6 mW, and a time constant of 0.01 ms. SP-PLP-ESR measurements were carried out at the magnetic field positions *H*(fix,pos) and *H*(fix,neg), indicated by the full and dash-dotted arrow, respectively.

The essential advantages of SP-PLP-ESR over SP-PLP-NIR should be noted: (i) the termination kinetics is analyzed by directly monitoring the time evolution of radical concentration. and (ii) the experiments may be easily extended to fairly low temperatures. It appears to be a matter of priority to advance the SP-PLP-ESR technique such that also polymerizations of monomers with higher k_t may be accurately measured. Chain-length-averaged k_t values for *n*-BMA and *t*-BMA[28] indicate that these two monomers should be good candidates for such studies with improved time resolution of the SP-PLP-ESR experiment. The present paper details the results for $k_t^{1,1}$, α_s, α_l, and i_c obtained for *n*-BMA and *t*-BMA by measuring the time evolution of c_R after SP initiation with particular emphasis on the time range immediately after firing the laser pulse in which short-chain radicals are terminating.

Experimental Section

The ESR spectra were recorded on a Bruker Elexsys E 500 series cw-ESR spectrometer for sample volumes of 0.05 mL in quartz tubes of 3 mm o.d. and 2 mm i.d.. The tubes were fitted into a resonator cavity equipped with a grid through which the sample was irradiated with a COMPex 102 excimer laser (Lambda Physik) operated on the XeF line (351 nm) at a laser energy of about 30 mJ/pulse. The ESR spectrometer and the laser source were synchronized by a pulse generator (Scientific Instruments 9314). Temperature control in the range −30 to +60 °C was achieved via an ER 4131VT unit (Bruker) by purging the sample cavity with nitrogen.

The monomers *n*-BMA and *t*-BMA (>99.5%, stabilized with hydroquinone monomethyl ether, Fluka) were purified by passing through a column filled with inhibitor remover (Aldrich). Dissolved oxygen was removed by several freeze−pump−thaw cycles. The photoinitiator α-methyl-4(methylmercapto)-α-morpholinopropiophenone (MMMP, 98%, Aldrich) was used as received at initial concentrations of about 3×10^{-2} mol L^{-1}. The initiator was added to the degassed monomer in a glovebox under an argon atmosphere. The ESR tube was sealed with a plastic cap and with Parafilm and was protected from light prior to PLP.

As the first step of the SP-PLP-ESR experiment, an ESR spectrum was taken under pseudostationary PLP initiation conditions using the signal channel (SC) detection system. Such a spectrum recorded with a laser pulse repetition rate of 20 Hz on *n*-BMA at −10 °C is depicted in Figure 1. The short sweep time of 10.5 s was selected to avoid significant monomer-to-polymer

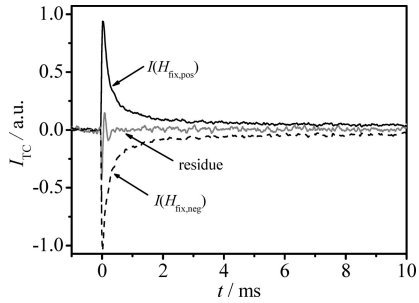

Figure 2. ESR intensity vs time traces for *n*-butyl methacrylate polymerization at −10 °C recorded after laser single pulse initiation ($t = 0$) at the constant magnetic field positions $H_{fix,pos}$ (full line) and $H_{fix,neg}$ (dashed line), as indicated in Figure 1. The sum of $I_{TC}(H_{fix,pos})(t)$ and $I_{TC}(H_{fix,neg})(t)$, i.e. the residue, is represented by the gray line.

conversion prior to the actual SP experiment. Via ESR spectra recorded prior to studying a polymerization system, the spectroscopic parameters, in particular, the modulation amplitude and the microwave energy (to avoid saturation) had to be optimized such that high signal-to-noise quality is reached. The first spectrum of each SP-PLP-ESR experimental series is used to identify the peak maximum positions for time-resolved measurements. The ESR spectrum in Figure 1 shows rather broad lines. Because of the short sweep time, the long-range hyperfine coupling with the γ-protons of the ester group is not resolved. Narrow ESR lines are obtained upon enhancing the sweep time by about 2 orders of magnitude.[29] The so-obtained highly resolved ESR spectrum of *n*-BMA macroradicals is in perfect agreement with the one reported by Kamachi and Kajiwara.[30] The magnetic field position, H(fix,pos), for time-resolved c_R detection after initiation by a single pulse was chosen to be the one of the intense outer line indicated by the full arrow in Figure 1. In contrast to the central line, this spectral component is not affected by the ESR spectrum of primary initiator-derived radicals.[29]

Mostly, also the time dependence at the position H(fix,neg) (see Figure 1) was measured. The detection system used for tracing ESR intensity at constant magnetic field (TC, time channel) in contrast to the signal channel (SC), where full ESR spectra are recorded, operates at a time resolution of 500 ns. In order to increase signal-to-noise quality, up to 30 individual intensity data points were accumulated, thus reducing the time resolution to about 15 μs. To further enhance signal quality, the data from 200 separate single pulse experiments were coadded. It was checked that the intensity (I_{TC}) vs time curves do not change with the number of applied pulses due to either monomer or initiator consumption. The overall monomer-to-polymer conversion after each experiment, i.e., after measuring an ESR spectrum and an SP-PLP trace, was estimated gravimetrically to be less than 10%. In this initial polymerization range, termination rate coefficients may be assumed to be independent of monomer conversion as is indicated by SP-PLP-NIR results.[28]

Shown in Figure 2 are ESR intensity traces recorded after SP initiation at $t = 0$ for an *n*-BMA polymerization at −10 °C. The curves were measured at the constant magnetic field positions $H_{fix,pos}$ (full dashed) and $H_{fix,neg}$ (dashed line) (see Figure 1). The residue (gray line), i.e., the sum of $I_{TC}(H_{fix,pos})(t)$ and $I_{TC}(H_{fix,neg})(t)$, coincides with the baseline at times t exceeding 1 ms after laser pulsing, which indicates that the traces are undisturbed and highly reproducible. For shorter times, $t < 1$ ms, after SP initiation, the residue exhibits a signal which is also seen in SP-PLP-ESR measurements at arbitrary magnetic field position, including regions beyond the absorption range of the different radical species. This signal is assigned to a perturbation of resonator quality by the laser pulse. The signal becomes negligible in situations of low laser energy being applied in conjunction with high initiator concentration, as was the case in the present study.

Quantitative Determination of Radical Concentrations. The determination of absolute radical concentrations is based on the proportionality between the double integral of the ESR (dispersion) spectrum, recorded on the signal channel (SC), $\int\int I_{SC}$, and the associated amount of spins in the system under investigation. At constant sample volume the correlation between $\int\int I_{SC}$ and radical concentration, c_R, reads

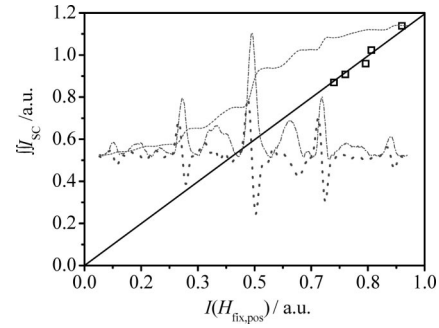

Figure 3. Correlation between ESR intensity at fixed magnetic field, $I_{SC}(H_{fix,pos})$, and the associated double integral of the ESR spectrum, $\int\int I_{SC}$. Included is an ESR spectrum of *tert*-butyl methacrylate macroradicals created by pulsed laser polymerization with a repetition rate of 20 Hz at −10 °C (dashed bold line) as well as the associated integral (dot-dashed line) and double integral (dashed line).

$$c_R = h_1 \iint I_{SC} \tag{4}$$

As eq 4 holds irrespective of the type of radical species, the setup-specific proportionality factor h_1 may be obtained by calibration via the stable radical 2,2,6,6-tetramethylpiperidyl-1-oxyl (TEMPO, 99%, Aldrich) dissolved in the monomer under investigation.[31,32] As time-resolved ESR analysis is carried out via the intensity at fixed magnetic field, $I_{SC}(H_{fix,pos})$, a second calibration is required which correlates $I_{SC}(H_{fix,pos})$ to the double integral:

$$\iint I_{SC} = h_2 I_{SC}(H_{fix,pos}) \tag{5}$$

To perform the calibration according to eq 5, different macroradical concentrations were produced by varying laser pulse energy in pseudostationary polymerizations. Plotted in Figure 3 are double integral values, $\int\int I_{SC}$, vs the associated $I_{SC}(H_{fix,pos})$ data for *t*-BMA polymerizations at −10 °C using different radical concentrations. The linear correlation allows for deducing the proportionality constant h_2. Included in this figure are the ESR spectrum, the associated integral, and the double integral. The calibration in Figure 3 refers to the SC detection system. As time-channel (TC) detection is used for the measurement of the SP-PLP-ESR traces, a third calibration step has been performed, in which the sensitivities of the SC and TC detection systems are correlated (eq 6), again via measurements on TEMPO dissolved in the two butyl methacrylate monomers.

$$\iint I_{SC} = h_3 \iint I_{TC} \tag{6}$$

The two double integral intensities were found to be proportional to each other. The proportionality factor, h_3, may be obtained more directly, although with lower accuracy, by correlating $I_{SC}(H_{fix,pos})$ with $I_{TC}(H_{fix,pos})$ during a polymerization experiment. The ESR spectra of the stable radical TEMPO (10^{-5} mol L^{-1} in *t*-BMA) at −10 °C recorded via SC (full line) and TC (dashed line) detection are shown in Figure 4 together with the associated double integrals. The sensitivity of TC detection is by about a factor of 2 below the one of SC detection. The proportionality factor h_3 is valid for all polymerization temperatures used in the present study and is independent of TEMPO concentration. Moreover, no offset in magnetic field positions is seen in between the ESR spectra.

Combining eqs 4−6 results in the final expression for transformation of $I_{TC}(H_{fix,pos})(t)$ into $c_R(t)$ data:

$$c_R(t) = h_1 h_2 h_3 I_{TC}(H_{fix,pos})(t) \tag{7}$$

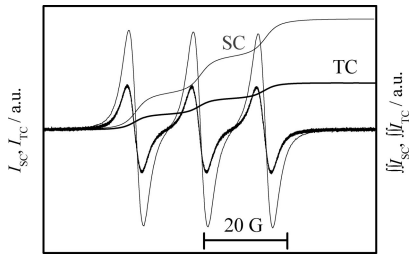

Figure 4. ESR spectrum and associated double integral for TEMPO (10^{-5} mol L^{-1} in *tert*-butyl methacrylate) at −10 °C measured via the signal channel (SC, full lines) and the time channel (TC, bold lines) detection, respectively.

with the proportionality factors h_1, h_2, and h_3 being deduced from the calibration procedures outlined above.

Determination of macroradical concentrations is assumed to be accurate within ±30%. Relative radical concentrations, $c_R(t)/c_R^0$, where c_R^0 is the initial radical concentration produced by the addition of the first *n*-BMA or *t*-BMA monomer to a primary initiator-derived radical, is accessible with higher accuracy, as $c_R(t)/c_R^0$ is directly obtained from the $I_{TC}(H_{fix,pos})$ trace without any calibration being involved. Integration of the spectra and fitting of kinetic expressions to $c_R(t)$ traces were carried out via the software package Origin7.1.

Data Fitting. Macroradical chain length, i, at time t after laser SP initiation may be expressed by $i = k_p c_M t$ (in case that chain transfer does not intervene). Implementing this relation into eq 2 followed by integration of the differential rate law for termination (eq 3) yields

$$\frac{c_R^0}{c_R(t)} - 1 = \frac{2k_t^{1,1} t c_R^0 t_p^{\alpha_s}}{1-\alpha_s} t^{1-\alpha_s} \qquad \text{for } i < i_c \tag{8}$$

and

$$\frac{c_R^0}{c_R(t)} - 1 = \frac{2k_t^0 c_R^0 t_p^{\alpha_l}}{1-\alpha_l} t^{1-\alpha_l} \qquad \text{for } i > i_c \tag{9}$$

where t_p is the mean time interval required for a single propagation step, i.e., $t_p = (c_M k_p)^{-1}$. In principle, the four parameters of the composite model for $k_t^{i,i}$, i.e., $k_t^{1,1}$, α_s, α_l, and i_c, may be deduced from plotting $\log(c_R^0/c_R(t) - 1)$ vs $\log t$. The two linear regimes, with slopes $(1 - \alpha_s)$ and $(1 - \alpha_l)$, respectively, should intersect at $\log t_c$. The associated crossover chain length is $i_c = k_p c_M t_c$. As will be shown further below, this approach provides access only to i_c and α_l, whereas less precise values are obtained for $k_t^{1,1}$ and α_s.[26,33] The reason behind this inaccuracy is the inadequate description of chain length immediately after applying the laser SP. The relation $i = k_p c_M t$ would imply $k_t^{1,1}$ to be infinite at $t = 0$.

A physically more realistic description is based on the relation $i = k_p c_M t + 1$, which however results in a more complicated expression for c_R as a function of t at $i < i_c$ (eq 10), as has been shown by Smith and Russell and has been tested by means of SP-PLP-ESR data for DMA, CHMA, and BzMA.[26,33]

$$\frac{c_R^0}{c_R(t)} - 1 = \frac{2k_t^{1,1} c_R^0 ((k_p c_M t + 1)^{1-\alpha_s} - 1)}{k_p c_M (1-\alpha_s)} \tag{10}$$

Equation 10 allows for an adequate description of termination of radicals with chain length $i < i_c$ and kinetic analysis of the short-chain regime, whereas eq 8 is restricted to longer chains, e.g., $i > 5$ in the case of *t*-BMA polymerization.[26] Application of eq 10, however, requires nonlinear fitting. Both approaches, i.e., regression via eq 8 or via eq 10, have been compared in ref 26. It turned out that eq 10 should be used for α_s and $k_t^{1,1}$ analysis, as has been done in the present study.

Smith and Russell also derived an exact solution, on the basis of $i = k_p c_M t + 1$, for the long-chain regime (eq 11).[33] This

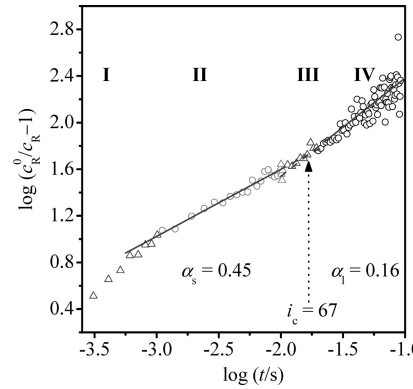

Figure 5. Plot of $\log(c_R^0/(c_R - 1))$ vs $\log t$ data as obtained via SP-PLP-ESR experiments on *tert*-butyl methacrylate at 50 °C. The full lines show the linear fits to the data in the short-chain ($5 < i < 50$) regime in segment II and the long-chain regime ($i > 100$) in segment IV. The data in segments I ($i < 5$) and III (triangles) were not used for regression; the entire data set refers to monomer conversions below 10%.

expression however turned out to be rather insensitive toward α_l determination.[26]

$$\frac{c_R^0}{c_R(t)} - 1 = \frac{2k_t^{1,1} c_R^0 ((i_c)^{1-\alpha_s} - 1)}{k_p c_M (1-\alpha_s)} - \frac{2k_t^{1,1} c_R^0 (i_c)^{1-\alpha_s}}{k_p c_M (1-\alpha_l)} + \frac{2k_t^0 c_R^0 (k_p c_M t + 1)^{1-\alpha_l}}{k_p c_M (1-\alpha_l)} \tag{11}$$

Actually, the analysis of the $c_R(t)$ traces for *n*-BMA and *t*-BMA polymerizations via eq 11 yields α_l values which are close to zero or even negative. This problem is not due to a failure of eq 11, but results from the changes in signal intensity at chain lengths well above i_c being too small as to allow for a reasonable fit of the data to eq 11. Thus, eq 9 was used for deducing α_l from the experimental data; i.e., α_l was determined from a $\log(c_R^0/c_R(t) - 1)$ vs $\log t$ plot, following the recommendation made by Russell et al.,[26] although α_l may be slightly overestimated by this procedure. The transition region between the long-chain and short-chain regimes (triangles in region III of Figure 5, see below) has not been included into the linear fitting.

To summarize, the linear fitting procedure according to eqs 8 and 9 provides access to i_c and α_l, whereas eq 10 is used for deducing $k_t^{1,1}$ and α_s. The propagation rate coefficients of *n*-BMA[34] and *t*-BMA,[35] which are required for data evaluation, were taken from literature PLP-SEC studies.

Results and Discussion

The procedure of deducing i_c and α_l is illustrated in Figure 5 by a $\log(c_R^0/c_R(t) - 1)$ vs $\log t$ plot of data from a *t*-BMA polymerization at 50 °C. The linear correlations for regions II and IV intersect in region III with the point of intersection yielding $\log t_c$. The crossover chain length, i_c, is estimated from $i_c = k_p c_M t_c + 1$. The exponent α_l is obtained from the slope $(1 - \alpha_l)$ within the long-chain-length regime IV. The $\log(c_R^0/c_R(t) - 1)$ vs $\log t$ plot affords for no satisfactory representation at short times t after applying the laser single pulse (segment I). The essential reason behind the curvature of the data toward small chain lengths, e.g., at $i < 5$, appears to be that eq 8 is based on the expression $i = k_p c_M t$. To at least partially avoid associated uncertainties, linear fitting in region II has been restricted to radicals with chain lengths $5 < i < 50$, whereas eq 9 was used at chain lengths above $i = 100$ (region IV). The data plotted in Figure 5 yield as composite-model parameters $\alpha_l = 0.16 \pm 0.05$ and $i_c = 67$ with the accuracy interval of i_c being nonsymmetric: −10 and +20.

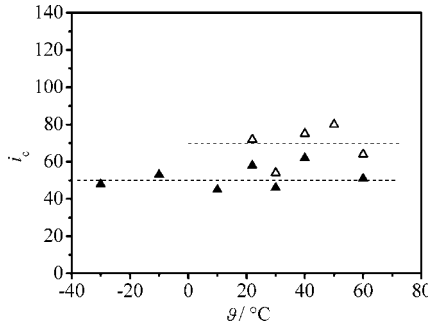

Figure 6. Temperature dependence of the crossover chain length, i_c, for polymerization of *n*-butyl methacrylate (*n*-BMA) (filled triangles) and *tert*-butyl methacrylate (*t*-BMA) (open triangles). The dashed lines represent the temperature-averaged values of $i_c = 50$ for *n*-BMA and $i_c = 70$ for *t*-BMA. The data refers to monomer conversions below 10%.

SP-PLP-ESR traces of *n*-BMA and *t*-BMA were recorded in the temperature range −30 to +60 °C. The i_c values determined for the different temperatures are plotted for both *n*-BMA and *t*-BMA in Figure 6. There is no indication of any temperature dependence of i_c. Despite the significant uncertainty in i_c determination, the values for *t*-BMA and *n*-BMA appear to be different. The temperature-averaged values, indicated by the dashed lines, are $i_c = 50$ for *n*-BMA (filled triangles) and $i_c = 70$ for *t*-BMA (open triangles).

In order to obtain the $k_t^{1,1}$ and α_s values referring to small-size radicals, the $c_R(t)$ data were fitted to eq 10 in the time interval $0 < t < t_c$. The first two data points measured immediately after applying the laser pulse, in the time range where c_R is still increasing, were not considered within the regression analysis. Whereas α_s is directly deduced from the fitting, $k_t^{1,1}$ is obtained in coupled form as $c_R^0 k_t^{1,1}$. Thus, the initial concentration of radicals formed by addition of the first monomer to the primary initiator-derived radicals, c_R^0, needs to be known. To deduce accurate $k_t^{1,1}$ values, the early data points taken immediately after applying the laser SP have to be measured with high time resolution. Otherwise, the maximum in the $I_{TC}(H_{fix,pos})(t)$ trace will be underestimated. For a rapidly decreasing quantity, such as the radical concentration, there is a tendency of determining too low values due to averaging over time *t*. This effect becomes negligible as soon as a sufficiently high time resolution is reached.[29]

A typical fit to eq 10 is exemplified by the $c_R^0/c_R(t) - 1$ vs *t* plot in Figure 7. The underlying $c_R(t)$ data were recorded during a laser SP-induced polymerization of *t*-BMA at 30 °C. The best fit is achieved with an exponent $\alpha_s = 0.65$. The sensitivity of the fitting procedure toward α_s is illustrated by curves referring to $\alpha_s = 0.55$ and $\alpha_s = 0.85$. Visual inspection of these curves tells that $\alpha_s = 0.65$, within the nonsymmetric error limits of +0.20 and −0.10, allows for an adequate representation of the chain-length dependence of the termination rate coefficient $k_t^{i,i}$ of radicals with chain lengths $i < i_c$.

The $c_R(t)$ data for *t*-BMA (open symbols) and *n*-BMA (filled symbols) polymerizations at temperatures between −30 and +60 °C were analyzed according to eqs 9 and 10. The resulting parameters α_s (squares) and α_l (diamonds), which partly are mean values from independent experiments, are depicted in Figure 8. The short-chain exponent, α_s, for *n*-BMA appears to be independent of temperature: $\alpha_s = 0.65 \pm 0.10$. With *t*-BMA it is less clear, whether or not α_s varies with temperature, but α_s seems to be below 0.65. The arithmetic mean value of α_s is obtained to be 0.56 ± 0.1 for *t*-BMA.

The α_l values determined via linear fitting (see Figure 5) are uncertain by ±0.05. No significant difference in the α_l values for *t*-BMA (open diamonds) and *n*-BMA (filled diamonds) is seen. Averaging the entire data set determined for the two butyl methacrylates within the experimental temperature range yields $\alpha_l = 0.20 \pm 0.05$ (see Figure 8).

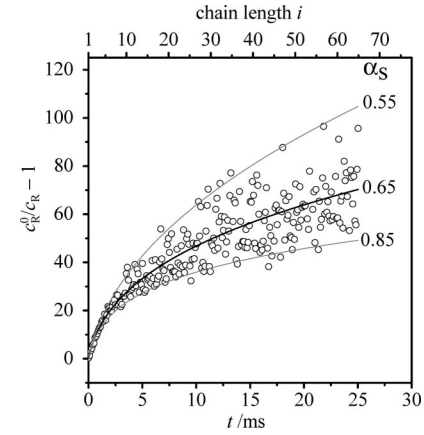

Figure 7. Plot of $c_R^0/c_R(t) - 1$ vs time *t* after laser single pulse initiation at $t = 0$ during a polymerization of *tert*-butyl methacrylate at 30 °C. The full line represents a fit of the experimental ESR-derived data to eq 10. The data refer to monomer conversions below 10%. Curves for $\alpha_s = 0.55$ and 0.85 are included to illustrate the data and fitting quality (see text).

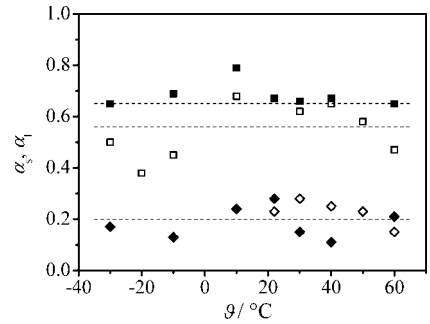

Figure 8. Temperature dependence of α_s (squares) and α_l (diamonds) values as obtained from ESR-derived radical concentrations measured during *n*-butyl methacrylate (*n*-BMA, filled symbols) and *tert*-butyl methacrylate (*t*-BMA, open symbols) polymerizations, respectively. α_s was determined via eq 10 for chain lengths up to 50 with *n*-BMA and up to 70 with *t*-BMA. The α_l values were obtained via the linear fitting approach using eq 9. The dashed lines indicate the mean values averaged over polymerization temperature.

The rate coefficient for termination of two radicals of chain length unity, $k_t^{1,1}$, was obtained as the second parameter from fitting the radical concentration data to eq 10 (see Figure 7). It should be noted that the $k_t^{1,1}$ values reported in the present paper refer to BMA polymerizations at very low degrees of monomer conversion with the polymer content being of the order of 5 wt %. For *t*-BMA polymerizations at temperatures of −10 °C and below, α_s was kept constant at 0.56 in order to avoid that, because of the correlation of $k_t^{1,1}$ and α_s, meaningless values of $k_t^{1,1}$ are deduced by a two-parameter fit of the low-temperature data which exhibit a larger scattering. No significant decrease in the quality of the fit was observed for this one-parameter fitting procedure compared to two-parameter regression.

Arrhenius plots of $k_t^{1,1}$ for *n*-BMA (filled circles) and *t*-BMA (open circles) are depicted in Figure 9. The individual activation energies, $E_A(k_t^{1,1})$, are 10.1 kJ mol^{-1} for *n*-BMA and 12.0 kJ mol^{-1} for *t*-BMA (dashed lines). As $k_t^{1,1}$ is assumed to be controlled by center-of-mass diffusion, it is gratifying to note that $E_A(k_t^{1,1})$ is close to the activation energy of monomer fluidity, which is about 10 kJ mol^{-1} for both monomers.[28] The $k_t^{1,1}$ values for *n*-BMA and *t*-BMA are sufficiently close to each other, such as to allow for a joint Arrhenius fit. The resulting dashed line is associated with an activation energy of $E_A(k_t^{1,1})$

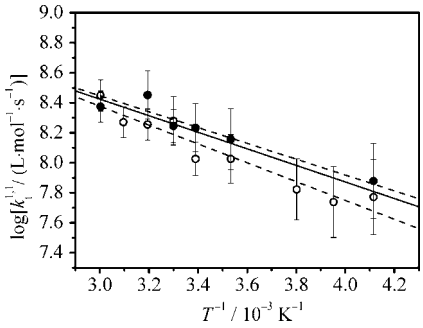

Figure 9. Arrhenius plot of the termination rate coefficient of two radicals of chain length unity, $k_t^{1,1}$. The $k_t^{1,1}$ data were obtained by fitting the radical concentration traces of *n*-butyl methacrylate (filled circles) and *tert*-butyl methacrylate (open circles) to eq 10 (for details see text). The full line represents an Arrhenius fit to the joint $k_t^{1,1}$ data set for *n*-BMA and *t*-BMA.

$= 10.5 \pm 2$ kJ mol^{-1}. It should be noted that the two $E_A(k_t^{1,1})$ values are well below the previously reported $E_A(\langle k_t \rangle_{SD})$ values of about 20 kJ mol^{-1}, which are the activation energies for k_t at low degrees of monomer conversion, where segmental diffusion is rate controlling. The reason behind this discrepancy is not yet clear. Experiments with further improved signal-to-noise quality may answer the question of whether one of the composite model parameters is temperature dependent, which could account for the difference in the two types of activation energies.

The final set of composite-model parameters obtained for *n*-BMA and *t*-BMA bulk polymerization is summarized in Table 1.

In what follows, the composite model parameters for *n*-BMA and *t*-BMA will be analyzed by assuming termination to be controlled by center-of-mass diffusion at short chain lengths and by segmental diffusion at long chain lengths. The data will be compared to previously reported SP-PLP-ESR data for DMA, BzMA, and CHMA bulk polymerizations at 0 °C[26] and to experimental data for the chain-length dependence of the diffusion coefficient of oligomeric *n*-BMA species dissolved in *n*-BMA as reported by Griffiths et al.[36]

The power-law exponent for long-chain radicals in *n*-BMA and *t*-BMA homopolymerizations is found to be $\alpha_l = 0.20$. In view of the fact that linear fitting to eq 9 may result in a slight overestimation of α_l, this value may be considered to be very close to the theoretically predicted exponent of $\alpha_l = 0.16$ for long entangled chains.[7] Very similar numbers for α_l, between 0.18 and 0.21, have been deduced in earlier SP-PLP-ESR experiments of our group on DMA, BzMA, and CHMA bulk homopolymerizations.[26] For styrene, Olaj and Vana observed an α_l value of 0.18 at 20 °C. The authors reported a lowering of α_l to ~0.10 at 70 °C, which was assigned to a decrease in solvent quality toward increasing temperature.[37] Within our present study, no such variation of α_l with temperature could be safely established for the temperature range −30 to 60 °C.

The crossover chain length i_c characterizes the radical size from which on two radicals may get entangled and thus experience a significantly enhanced contact time as compared to contact times of radicals with chain lengths $i < i_c$. As is indicated by the higher glass transition temperatures of polymethacrylates, these polymers exhibit lower chain flexibility than polyacrylates and thus should be less capable of forming entanglements. Within the methacrylate family, higher i_c is anticipated for monomers with bulky ester groups. According to this argument, the crossover chain length for *t*-BMA, $i_c = 70$, exceeds the one for *n*-BMA, $i_c = 50$, reflecting the higher steric demand of a *tert*-butyl group as compared to an *n*-butyl group. Higher chain flexibility is also indicated by the propagation rate coefficient under otherwise identical reaction conditions being larger for *n*-BMA than for *tert*-BMA. The effect of chain flexibility on the propagation rate coefficient results from hindrance of internal rotational motion of the transition structure for propagation. Reduced hindrance goes with an enhanced pre-exponential factor of the propagation rate coefficient, as is discussed in more detail elsewhere.[28,38]

The crossover chain length of DMA, $i_c = 50$, is identical to the one measured for *n*-BMA which may indicate that chain stiffness is essentially determined by the type of side-chain segments which sit next to the backbone. The similarity of i_c for DMA and *n*-BMA may however also be understood by assuming that the reduction in flexibility associated with the large dodecyl side chain is compensated by the fluidizing action of this longer alkyl moiety which serves as some kind of "internal" solvent. That such an internal fluidizing action plays a role is also indicated by the relatively large value of $i_c = 100$ reported for methyl methacrylate.[21] The methyl ester moiety of MMA should not be capable of providing any substantial solvent quality.

Relatively large crossover chain lengths, of about $i_c = 90$, have been found for two methacrylates with cyclic ester groups, CHMA and BzMA (see Table 2).[26] The cyclic alkyl ester groups thus appear to enhance chain stiffness. That the i_c values for CHMA and BzMA even exceed i_c of *t*-BMA may serve as an indication of significant mutual interactions of the cyclic moieties during segmental reorientation of the associated polymeric chains. The crossover chain length of methacrylate monomers of similar ester size appears to increase along the series *n*-alkyl < *sec*-alkyl < *tert*-alkyl < cyclic.

It needs to be tested whether this sequence applies also to other families, e.g., to the acrylates. So far, three *n*-alkyl esters have been studied. As is to be expected from the chain-flexibility argument, the i_c values for methyl,[17] butyl,[18] and dodecyl acrylate[17] polymerization are significantly below the ones for alkyl methacrylates. They range from 20 to 30 with the lowest number ($i_c \sim 20$) being found for dodecyl acrylate,

Table 1. Summary of the Composite-Model Parameters Obtained in This Work

	i_c	α_s	α_l	$k_t^{1,1}$(0 °C)/L mol s^{-1}	$E_A(k_t^{1,1})$/kJ mol^{-1}
n-BMA	50 ± 15	0.65 ± 0.15	0.20 ± 0.05	$1.3 \times 10^8 \pm 3 \times 10^7$	10.1 ± 2
t-BMA	70 ± 15	0.56 ± 0.15	0.20 ± 0.05	$9.1 \times 10^7 \pm 3 \times 10^7$	12.0 ± 2

Table 2. Comparison of $k_t^{1,1}$ Values Obtained for Bulk Polymerizations of Alkyl Methacrylates at 0 °C[a]

	n-BMA	*t*-BMA	BzMA	DMA	MMA
$k_t^{1,1}$/L mol^{-1} s^{-1}	1.3×10^8	9.1×10^7	3×10^7	1×10^7	4.7×10^8
$\eta/\eta_{n\text{-BMA}}$	1	1	1.4	4.4	0.6
$r_s/r_{s,n\text{-BMA}}$	1	~1[b]	~1.4[b]	1.8	0.6
$R_c/R_{c,n\text{-BMA}}$	1	~0.7	~0.4	0.6	~1.3
ref	this work, 28, 42	this work, 28, 42	26, 42	26, 42	21, 42

[a] Also contained are values of i_c, α_s, relative viscosity, and relative hydrodynamic monomer radius. The relative capture radii were calculated based on the $k_t^{1,1}$, η, and r_s data (for details see text). [b] The hydrodynamic radii were interpolated according to the number of atoms in the monomer; the $k_t^{1,1}$ value for MMA was determined at 80 °C via RAFT-CLD-T and extrapolated to 0 °C using $E_A = 10$ kJ mol^{-1}.

the monomer with the largest alkyl ester side chain, and vice versa ($i_c \sim 30$ for methyl acrylate). This finding additionally supports the argument of a long alkyl ester group acting as an "internal" solvent and enhancing the flexibility of the polymeric chain.

Within a recent SP-PLP-NIR study, mean values of termination rate coefficients for the chain-length interval $1 < i < 1000$ have been determined for *n*-BMA and *t*-BMA bulk polymerization at 2000 bar. The so-obtained numbers have been obtained at low monomer-to-polymer conversions where approximately constant plateau values of k_t are found. They are denoted as $\langle k_t \rangle_{SD}$, thus indicating that termination occurs under segmental diffusion control.[28] The activation energies of $\langle k_t \rangle_{SD}$ have been reported to be 18.7 kJ mol^{-1} for *n*-BMA and 24.4 kJ mol^{-1} for *t*-BMA,[28] thus clearly exceeding the activation energy for $k_t^{1,1}$ obtained within the present study. The difference in the activation energies $E_A(k_t^{1,1})$ and $E_A(\langle k_t \rangle_{SD})$ provides further evidence for different modes of diffusion control being operative in the initial region of short contact, $i < i_c$, from which $E_A(k_t^{1,1})$ is deduced, and in the chain-length region $i > i_c$, which is primarily probed by the SP-PLP-NIR experiment thus providing a value for $E_A(\langle k_t \rangle_{SD})$.

The sizes of $k_t^{1,1}$ as well as of α_s are determined by center-of-mass diffusivity of small radicals. The associated rate coefficient, k_{diff}, may be estimated from the Smoluchowski equation:[39]

$$k_{diff} = 2\pi N_A D_s R_c \tag{12}$$

where N_A is the Avogadro number, D_s is the mutual diffusion coefficient of the reacting species, and R_c is the capture radius. For reaction of two radicals of identical chain length *i*, with D^i being the center-of-mass diffusion coefficient of an individual radical, D_s is equal to $2D^i$. D^i may be represented by the Stokes−Einstein equation:

$$D^i = \frac{k_B T}{6\pi r_{si} \eta} \tag{13}$$

where k_B is the Boltzmann constant and r_{si} the hydrodynamic radius of a radical of chain length *i*. Equation 12 in conjunction with eq 13 suggests that k_{diff} and thus k_t should be independent of chain length in the case that R_c and r_{si} vary with chain length in a very similar or even identical fashion. Quenching experiments on polystyrene,[40] however, revealed that R_c is almost independent of the degree of polymerization in the short-chain regime. Thus, the chain-length dependence of $k_{t,diff}$ and thus of $k_t^{i,i}$ should be governed by D^i. At infinite dilution, the center-of-mass diffusion coefficient for ideal random coils should scale with chain length according to $D^i \propto i^{-0.5}$.[6] In case that excluded volume effects are considered, the correlation becomes $D^i \propto i^{-0.6}$.[41] The experimental values provided within the present study, $\alpha_s = 0.65$ for *n*-BMA and $\alpha_s = 0.56$ for *t*-BMA, are close to the predicted value of $\alpha_s = 0.6$. The chain-length dependence of D^i has been determined for *n*-BMA oligomers with chain lengths up to $i = 10$ in solution of monomeric *n*-BMA. The resulting relation is $D^i \propto i^{-0.66}$ with the exponent almost exactly matching the α_s value determined in our SP-PLP-ESR experiments on the same monomer.[36] For the bulk homopolymerizations of BzMA, CHMA, and DMA, SP-PLP-ESR experiments at 0 °C have provided α_s values of 0.50, 0.50, and 0.64, respectively.[26] Our results are consistent with these findings in that α_s is higher for *n*-BMA where the pendant group is linear, as with DMA, and in that α_s is lower in case of *t*-BMA where the pendant group is spherical, as with BzMA and CHMA.

The maximum value of $k_t^{1,1}$ is given by the so-called diffusion limit, with the associated number being estimated from $k_{t,max}^{1,1} = 4RT/(3\eta)$ which relation is obtained by combination of eqs 12 and 13 assuming $R_c = 2r_{s1}$. The monomer viscosities from ref 28 yield $k_{t,max}^{1,1} \approx 3 \times 10^9$ L mol^{-1} s^{-1} at 0 °C for both *t*-BMA and *n*-BMA. The diffusion limiting value, $k_{t,max}^{1,1}$, exceeds $k_t^{1,1}$ by more than 1 order of magnitude. This difference reflects the fact that the capture radius for the termination reaction is governed by the reactive center at the radical site rather than by the entire radical, i.e., $r_{s1} \gg R_c$, even at $i = 1$.

It is instructive to correlate the $k_t^{1,1}$ values with the associated monomer viscosities and hydrodynamic radii. A set of $k_t^{1,1}$ values deduced from SP-PLP-ESR experiments on bulk alkyl methacrylate polymerizations at 0 °C is collated in Table 2. Also listed in Table 2 are relative monomer viscosities and relative hydrodynamic radii (both with respect to the numbers for *n*-BMA). As viscosities were not always available for 0 °C, the relative viscosities in Table 2 partly refer to higher temperature. The hydrodynamic radii of *t*-BMA and BzMA were estimated from the r_s values for *n*-alkyl methacrylates reported in ref 42. This literature data are from light scattering experiments.

Combination of eqs 12 and 13, with k_{diff} being identified with $k_t^{1,1}$, yields eq 14:

$$R_c = \text{const}_T r_{s1} k_t^{1,1} \eta \tag{14}$$

where const_T is a proportionality factor which only depends on temperature. Equation 14, e.g., allows for deducing relative capture radii, $R_c/R_{c,n\text{-BMA}}$, from relative $k_t^{1,1}$ values, $k_t^{1,1}/k_{t,n\text{-BMA}}^{1,1}$, measured for a monomer of interest at identical temperature and with the associated relative values of hydrodynamic radius, $r_{s1}/r_{s1,n\text{-BMA}}$, and of viscosity, $\eta\ /\eta_{n\text{-BMA}}$, being known from independent experiments. The resulting numbers are listed in Table 2. Whereas the $k_t^{1,1}$ values of DMA and the two butyl methacrylates differ by about 1 order of magnitude, the capture radii are very similar. The differences in $k_t^{1,1}$ thus are predominantly due to dissimilar monomer viscosities and hydrodynamic radii. The slight differences in R_c between DMA and BzMA as well as between *n*-BMA and *t*-BMA are not considered to be significant in view of the accuracy of SP-PLP-ESR determination of $k_t^{1,1}$. The differences between DMA and BMA may however reflect some shielding of the radical center by the large ester groups of DMA, which results in a lowering of the capture radius. Along the same line of arguments, the relative capture radius of MMA should be enhanced, as the shielding potential of the methyl ester group will be minor. This is indeed what is seen in Table 1. The $k_t^{1,1}$ value for methyl methacrylate (MMA) bulk polymerization has been determined via RAFT-CLD-T to be $\sim 1.2 \times 10^9$ L mol s^{-1} at 80 °C.[20] Arrhenius extrapolation to 0 °C, via $E_A(k_t^{1,1}) = 10$ kJ mol^{-1}, yields $k_t^{1,1} \approx 4.7 \times 10^8$ L mol s^{-1}. The $R_c/R_{c,n\text{-BMA}}$ values in Table 2 indicate a family type behavior with $k_t^{1,1}$ being essentially determined by monomer viscosity and hydrodynamic radius. This type of k_t behavior has been predicted by Russell in his theoretical study into methacrylate bulk polymerizations.[43]

The very few $k_t^{1,1}$ values, which are currently available for other types of monomers, such as acrylates and itaconates, suggest that the dependence of alkyl methacrylate $k_t^{1,1}$ on monomer viscosity and monomer size may not be sufficient for estimating $k_t^{1,1}$. A value of $k_t^{1,1}$ for butyl acrylate (BA) bulk polymerization was determined via SP-PLP-NIR-RAFT for 2000 bar and 60 °C.[18] Extrapolation to ambient pressure and 0 °C yields $k_t^{1,1}(\text{BA}) \approx 5 \times 10^8$ L mol s^{-1}, which number exceeds the value for *n*-BMA by about half an order of magnitude, although *n*-BMA and BA have almost identical bulk viscosities[44] and hydrodynamic radii. SP-PLP-ESR studies into DBI, on the other hand, yield $k_t^{1,1}$ values of the order of 10^5 L mol s^{-1}, which are far below the coefficients listed in Table 2. It appears unlikely that such an enormous difference in $k_t^{1,1}$ can be assigned entirely to effects of monomer size and viscosity.

The impact of chain dynamics and shielding needs to be further investigated in subsequent work on a range of monomers carrying out both bulk and solution polymerizations. Of particular interest are SP-PLP-ESR investigations into high-k_t monomers, such as MMA and styrene. Termination rate coefficients may strongly decrease toward higher monomer-to-polymer conversion due to the Norrish−Trommsdorff effect. For such gel-effect conditions rather high power law exponents of $k_t^{i,i}$, up to 2, may be obtained.[21,22,36,45−47] It appears to be a matter of priority to extend the SP-PLP-ESR methodology to studies into chain-length-dependent termination up to high degrees of monomer conversion. Such investigations should provide a fundamental understanding of the dependence of k_t on both chain length and degree of monomer conversion. Further extension of the method should encompass detailed studies into systems containing more than one type of radicals, such as acrylates, where secondary and tertiary radicals are simultaneously present in the polymerizing medium.[48,49]

Conclusions

Chain-length-dependent termination kinetics of *n*-BMA and *t*-BMA bulk polymerization was investigated at low monomer-to-polymer conversions and temperatures between −30 and +60 °C via SP-PLP-ESR. Experiments with time resolution up to 15 μs enabled kinetic analysis in the short-chain regime which is less easily accessible by SP-PLP-NIR measurements. The experimental results confirm the validity of the so-called composite model for representing the decrease of $k_t^{i,i}$ with radical chain length i. For both monomers the composite-model parameters i_c, α_s, α_l, and $k_t^{1,1}$ were determined. The activation energy of the rate coefficient of termination for two radicals of chain length unity, $k_t^{1,1}$, is in close agreement with the temperature dependence of monomer fluidity. This finding indicates that $k_t^{1,1}$ is controlled by center-of-mass diffusion. Within the alkyl methacrylate family, the composite-model parameters are close to each other, with the exception of the crossover chain length, i_c. The differences in i_c are assigned to differences in chain flexibility.

Acknowledgment. Financial support by the Deutsche Forschungsgemeinschaft within the European Graduate School "Microstructural Control in Free-Radical Polymerization" (GRK 585) and a fellowship (to P.H.) from the Fonds der Chemischen Industrie are gratefully acknowledged. The authors are grateful to Prof. F. Meyer (Institute for Inorganic Chemistry, University of Göttingen) for providing the opportunity of using the ESR spectrometer in his laboratory.

References and Notes

(1) Buback, M.; Egorov, M.; Gilbert, R. G.; Kaminsky, V.; Olaj, O. F.; Russell, G. T.; Vana, P.; Zifferer, G. *Macromol. Chem. Phys.* **2002**, *203*, 2570–2582.
(2) Norrish, R. G. W.; Smith, R. R. *Nature (London)* **1942**, *150*, 336–3367.
(3) Trommsdorff, E.; Köhle, H.; Lagally, P. *Makromol. Chem.* **1948**, *1*, 169–198.
(4) Barner-Kowollik, C.; Buback, M.; Egorov, M.; Fukuda, T.; Goto, A.; Olaj, O. F.; Russell, G. T.; Vana, P.; Yamada, B.; Zetterlund, P. *Prog. Polym. Sci.* **2005**, *30*, 605–643.
(5) Smith, G. B.; Russell, G. T.; Heuts, J. P. A. *Macromol. Theory Simul.* **2003**, *12*, 299–314.
(6) Kirkwood, J. G.; Riseman, J. *J. Phys. Chem.* **1948**, *16*, 565–573.
(7) Friedman, B.; O'Shaughnessy, B. *Macromolecules* **1993**, *26*, 5726–5739.
(8) Khokhlov, A. R. *Makromol. Chem., Rapid Commun.* **1981**, *2*, 633–636.
(9) Olaj, O. F.; Zifferer, G. *Macromol. Chem., Rapid Commun.* **1982**, *3*, 549–556.
(10) Vana, P.; Davis, T. P.; Barner-Kowollik, C. *Macromol. Rapid Commun.* **2002**, *23*, 952–956.
(11) Olaj, O. F.; Bitai, I.; Hinkelmann, F. *Macromol. Chem.* **1987**, *188*, 1689–1702.
(12) Beuermann, S.; Buback, M.; Davis, T. P.; Gilbert, R. G.; Hutchinson, R. A.; Olaj, O. F.; Russell, G. T.; Schweer, J.; van Herk, A. M. *Macromol. Chem. Phys.* **1997**, *198*, 1545–1560.
(13) Buback, M.; Hippler, H.; Schweer, J.; Vögele, H.-P. *Makromol. Chem., Rapid Commun.* **1986**, *7*, 261–265.
(14) Buback, M.; Junkers, T.; Vana, P. *Macromol. Rapid Commun.* **2005**, *26*, 796–802.
(15) Theis, A.; Feldermann, A.; Charton, N.; Stenzel, M. H.; Davis, T. P.; Barner-Kowollik, C. *Macromolecules* **2005**, *38*, 2595–2605.
(16) Theis, A.; Davis, T. P.; Stenzel, M. H.; Barner-Kowollik, C. *Macromolecules* **2005**, *38*, 10323–10327.
(17) Buback, M.; Hesse, P.; Junkers, T.; Theis, T.; Vana, P. *Aust. J. Chem.* **2007**, *60*, 779–787.
(18) Junkers, T.; Theis, A.; Buback, M.; Stenzel, M. H.; Davis, T. P.; Vana, P.; Barner-Kowollik, C. *Macromolecules* **2005**, *38*, 9497–9508.
(19) Theis, A.; Feldermann, A.; Charton, N.; Davis, T. P.; Stenzel, M. H.; Barner-Kowollik, C. *Polymer* **2005**, *46*, 6797–6809.
(20) Johnston-Hall, G.; Theis, A.; Monteiro, M. J.; Davis, T. P.; Stenzel, M. H.; Barner-Kowollik, C. *Macromol. Chem. Phys.* **2005**, *206*, 2047–2053.
(21) Johnston-Hall, G.; Stenzel, M. H.; Davis, T. P.; Barner-Kowollik, C.; Monteiro, M. J. *Macromolecules* **2007**, *40*, 2730–2736.
(22) Johnston-Hall, G.; Monteiro, M. J. *Macromolecules* **2008**, *41*, 727–736.
(23) Barner-Kowollik, C.; Buback, M.; Charleux, B.; Coote, M. L.; Drache, M.; Fukuda, T.; Goto, A.; Klumperman, B.; Lowe, A. B.; McLeary, J. B.; Moad, G.; Monteiro, M. J.; Sanderson, R. D.; Tonge, M. P.; Vana, P. *J. Polym. Sci., Part A: Polym. Chem.* **2006**, *44*, 5809–5831.
(24) Buback, M.; Egorov, M.; Junkers, T.; Panchenko, E. *Macromol. Rapid Commun.* **2004**, *25*, 1004–1009.
(25) Buback, M.; Egorov, M.; Junkers, T.; Panchenko, E. *Macromol. Chem. Phys.* **2005**, *206*, 333–341.
(26) Buback, M.; Müller, E.; Russell, G. T. *J. Phys. Chem. A* **2006**, *110*, 3222–3230.
(27) Junkers, T. PhD Thesis, Göttingen, **2006**.
(28) Buback, M.; Junkers, T. *Macromol. Chem. Phys.* **2006**, *207*, 1640–1650.
(29) Barth, J. Diploma Thesis, Göttingen, **2008**.
(30) Kamachi, M.; Kajiwara, A. *Macromol. Symp.* **2002**, *179*, 53–74.
(31) Tonge, M. P.; Kajiwara, A.; Kamachi, M.; Gilbert, R. G. *Polymer* **1998**, *39*, 2305–2313.
(32) Kubota, N.; Kajiwara, A.; Zetterlund, P. B.; Kamachi, M.; Treurnicht, J.; Tonge, M. P.; Gilbert, R. G.; Yamada, B. *Macromol. Chem. Phys.* **2007**, *208*, 2403–2411.
(33) Smith, G. B.; Russell, G. T. *Z. Phys. Chem. (Munich)* **2005**, *219*, 295–323.
(34) Beuermann, S.; Buback, M.; Davis, T. P.; Gilbert, R. G.; Hutchinson, R. A.; Kajiwara, A.; Klumperman, B.; Russell, G. T. *Macromol. Chem. Phys.* **2000**, *201*, 1355–1364.
(35) Pascal, P.; Winnik, M. A.; Napper, D. H.; Gilbert, R. G. *Makromol. Chem., Rapid Commun.* **1993**, *14*, 213–215.
(36) Griffiths, M. C.; Strauch, J.; Monteiro, M. J.; Gilbert, R. G. *Macromolecules* **1998**, *31*, 7835–7844.
(37) Olaj, O. F.; Vana, P. *J. Polym. Sci., Polym. Chem. Ed.* **2000**, *38*, 697–705.
(38) Beuermann, S.; Buback, M.; Hesse, P.; Lacík, I. *Macromolecules* **2006**, *39*, 184–193.
(39) von Smoluchowski, M. *Z. Phys. Chem.* **1917**, *92*, 129–168.
(40) Strukelj, M.; Martinho, J. M. G.; Winnik, M. A. *Macromolecules* **1991**, *24*, 2488–2492.
(41) *Principles of Polymer Chemistry*; Flory, P. J., Ed.; Cornell University Press: Ithaca, NY, 1953.
(42) Mahabadi, H. K. *Makromol. Chem., Macromol. Symp.* **1987**, *10−11*, 127–150.
(43) Russell, G. T. *Macromol. Theory Simul.* **1995**, *4*, 549–576.
(44) Safety sheet butyl acrylate, Merck, **2004**.
(45) Brown, W.; Zhou, P. *Macromolecules* **1989**, *22*, 4031–4039.
(46) de Gennes, P. G. *J. Chem. Phys.* **1971**, *55*, 572–579.
(47) de Gennes, P. G. *J. Chem. Phys.* **1982**, *76*, 3322–3326.
(48) Buback, M.; Hesse, P.; Junkers, T.; Sergeeva, T.; Theis, T. *Macromolecules* **2008**, *41*, 288–291.
(49) Willemse, R. X. E.; van Herk, A. M.; Panchenko, E.; Junkers, T.; Buback, M. *Macromolecules* **2005**, *38*, 5098–5103.

MA802078G